Bandgap recovery and electron doping on cleaved [100] surfaces of divalent semi-metal hexaborides

J. D. Denlinger*, J. A. Clack, J. W. Allen, G.-H. Gweon
Department of Physics, Universtiy of Michigan, Ann Arbor, MI 48109-1120

D. M. Poirier‡, C. G. Olson
Ames Laboratory, Iowa State University, Ames, IA 50011

J. L. Sarrao†, Z. Fisk
National High Magnetic Field Lab and Dept. of Physics, Florida State University, Tallahassee, FL 32316

(December 2, 2024)

We present the first experimental view of the global band structure of the surprising divalent hexaborides. An unexpected and dramatic difference between the electronic structure observed for a region modified by the surface and that expected for the bulk highlights the fragility of the X-point band overlap that is thought to underlie the many novel electronic properties of these materials.

PACS numbers: 79.61.-i, 71.55.Ak, 75.30.-m

An oddity common to their electronic structures is thought to underlie various novel properties of the AB_6 hexaboride compounds with divalent element A. The crystal structure consists of B_6 boron octahedra at the centers and A atoms at the corners of a cubic unit cell. The simplest chemical bonding model predicts insulators, with two A-electrons per formula unit filling a boron-based valence band that is separated by a gap from an A-based conduction band. However, band structure calculations [1,2] have shown the possibility that the gap is closed by a small accidental overlap of bands at the cubic Brillouin zone X point, resulting in small hole and electron pockets which must have equal k-space volumes for a stoichiometric sample. Bandgap loss is very sensitive to the relative lengths of the intra- and inter-octahedral boron bonds, characterized by a structure parameter 'x' which is not symmetry determined [2]. The semi-metal possibility underlies various models to explain highly unusual properties that involve metallicity, a strong interplay of electrical transport and ferromagnetism [3–7] in EuB_6, anomalous transport properties [8] below a temperature of 1K in SrB_6, and most recently, unusual magnetic properties of $Ca_{0.995}La_{0.005}B_6$ that have been interpreted as showing a novel low moment, high Curie temperature ferromagnetic state [9]. Some models [10–12] for $Ca_{0.995}La_{0.005}B_6$ entail an excitonic instability of the overlapping X-point bands of the un-doped system. Evidence for pieces of Fermi surface (FS) due to small carrier pockets has been provided by de Haas van Alphen (dHvA) [13,14] and Shubnikov de Haas (SdH) [15] studies of XB_6 with X=Eu, Sr or Ca, but no experimental validation of the predicted global band structure has yet been reported. FS fine structures due to the spin-orbit interaction and to crossing hole-electron band mixing away from the high symmetry axes have also been predicted [16,17] but not yet observed.

Angle resolved photoemission spectroscopy (ARPES) provides a FS probe complementary to dHvA and SdH with the advantages that one obtains directly the overall shape and Brillouin zone position of the FS, and that one easily distinguishes whether holes or electrons have been observed. Disadvantages are that there is much less precision in determining the pocket sizes and, so far as studies of bulk electronic structure are concerned, that the method probes a region near the surface. We report here ARPES data for EuB_6 and SrB_6 that give the first direct view of the global band structure of divalent hexaborides, broadly as predicted by theory, but with the great surprise of a 1 eV X-point bandgap separating a filled "hole" band from a relatively large X-point electron pocket whose FS shape breaks cubic symmetry perpendicular to the surface. We speculate that cleaving produces an electron rich surface region with an X-point bandgap involving a variation from bulk to surface of the x-parameter value. The great sensitivity of the bandgap to the x-parameter may play a role in bulk properties as well.

The single crystal samples were grown from an aluminum flux using SrB_6 or EuB_6 powders prepared by boro-thermally reducing SrO and Eu_2O_3, respectively, a method shown to yield high quality with regard to both structure and chemical composition [8]. The ARPES was performed at the Ames/Montana beamline of the Synchrotron Radiation Center (SRC) at the University of Wisconsin. Samples oriented by Laue diffraction were cleaved in situ to reveal a [100] surface just before the measurement, which was done at a sample temperature of 20 K and in a vacuum chamber at pressure $\approx 4\times10^{-11}$ Torr. Monochromatized photons of energy $h\nu$ between 22 eV and 35 eV were used for the data reported here. The

Fermi energy (E_F) and instrumental resolution were calibrated with a reference spectrum taken on a sputtered Pt foil. The instrumental resolution ΔE was 130 meV and 170 meV FWHM for the spectra and maps, respectively, and the angular resolution for the electron spectrometer was $\pm 1^\circ$, which amounts to 6% of the distance from Γ to X in the simple cubic Brillouin zone.

To obtain ARPES FS maps the kinetic energy of the analyzer was fixed to correspond to the Fermi energy E_F and the analyzer was rotated away from the normal to the sample surface in two perpendicular directions by angles θ, ϕ in steps of 1°while the ARPES intensity was recorded. Basic photoemission theory shows that this angle variation corresponds to moving in k-space on a spherical surface having a radius that depends on the kinetic energy and hence on the photon energy and binding energy of the photohole. Because of translational invariance parallel to the surface the photohole momentum parallel to the surface is the same as that of the photoelectron and so is determined unambiguously by these angles and the kinetic energy of the photoelectron. [18] Perpendicular to the surface, the relation between photoelectron and photohole momenta involves also the surface potential and we find that the relation based on the commonly used ansatz [18] of photoelectron plane waves traversing an "inner potential step" V_0 yields internally consistent results if V_0=11.2 eV. For this value of V_0 the arc for hν=30 eV passes through the X point.

Fig. 1 shows as reverse gray scale images the measured energy distribution curves (EDC's) for hν=29.5 eV along Γ-X over a binding energy range to 9 eV below the Fermi energy E_F. For SrB_6 the data are shown for Γ-X directions both parallel and perpendicular to the photon electric vector. For both materials, the parallel polarization (panels (a) and (b)) clearly shows an X-point electron pocket discussed in detail below, but a boron band hole pocket is not observed. Overplotted are the boron bands calculated for SrB_6, but shifted to deeper binding energy by 1.5 eV relative to the electron pocket band, such that there is an ≈1-eV X-point bandgap. For reference, panel (d) of Fig. 1 shows the un-shifted bands compared to experimental peak positions with a vertical arrow to show the proposed 1.5 eV shift. Including the shift, and noting that a band dispersing to larger binding energy from $\Gamma \rightarrow$X appears only in the perpendicular polarization (panel (c)), all the major predicted dispersions can be identified, including that of the band that should give rise to the hole pocket. One now sees that the hole pocket is missing because the corresponding band lies well below E_F in both materials.

The top left panel of Fig. 2 shows for EuB_6 a FS map for hν=30 eV around the X-point, projected onto the k_x-k_y plane, parallel to the sample surface, with the k_x-k_y axes along Γ-X, X-M, respectively. The image in the figure is an interpolated version of the 19 × 21 pixels of the raw data. The X-point is located at the center of the image, which is clearly ellipsoidal. The bottom left panel shows EDC's along half the major axis of the ellipse. EDC's along the minor axis are very similar. The EDC's show that the FS arises from an essentially parabolic electron band. Fine structures predicted [16,17] for a crossing hole band are absent, as expected from the results of Fig. 1. The top and bottom right panels of Fig. 2 show equivalent results for SrB_6. Although the electron pocket is too small for its shape and center to be resolved, the map's intensity distributions along the k_x-k_y axes are asymmetric, consistent with a small ellipsoid. Detailed analysis of the EDC's and the image for EuB_6 yields the minor (a) and major (b) axes of the FS ellipse and the band effective masses m*, 2a = 0.235 (±0.025) $\mathring{A}^{-1}$ with m* = 0.21 (±0.03), 2b = 0.363 (±0.031) $\mathring{A}^{-1}$ with m*=0.5 (±0.06). For SrB_6 an indirect analysis method which assumes the same masses as for EuB_6 yields axes 2a = 0.102 (±0.031) $\mathring{A}^{-1}$ and 2b = 0.154 (±0.025) $\mathring{A}^{-1}$. These data for the parallel direction are generally consistent with theory for the electron band in both materials.

Fig. 3 (a,b) shows for EuB_6 the projection onto the k_x-k_z plane, i.e. a plane perpendicular to the sample surface, of an X-point FS image made by fixing one analyzer angle while varying the other angle and also the photon energy. Panel (b) shows the same data as panel (a), but normalized by the average intensity at each photon energy. Open dots in panel (b) show the k-points of the EDC's of Fig. 2 and of normal emission EDC's with varying hν, shown in panel (c). Panel (d) is an intensity representation of the EDC's in (c) normalized by the integrated spectral weight from 0.5 eV to E_F. The closed dots in (b) show FS points implied by E_F crossings in the EDC's. Rather than the expected elliptical solid of revolution, the FS is elongated along the surface normal into a sausage shape with elliptical cross-section and length 2c ≈ 0.6 $\mathring{A}^{-1}$. Because it is diffuse at small k_z and does not extend further in that direction, we cannot prove conclusively that the image of (b) closes at the low k_z end, but the closed boundary of the darkest inner part and the clear E_F crossing in the EDC's of (c) are very strong evidences for that interpretation. For the much smaller and hence poorly resolved FS of SrB_6 a k_x-k_z map is inconclusive but hints at a similar result. This FS breaks the four-fold rotational symmetry of the cubic X-M plane. Taking the FS volume as ≈2cπab the electron density is $3abc/2\pi^2$ (2 spin states/orbital, 1/2 the volume of 6 sausages per unit cell, and $1/(2\pi)^3$ states per unit volume in k-space, per unit volume in real space), giving $\approx 1 \times 10^{21}/cm^3$ for EuB_6.

We ascribe the observed electronic structure to a region modified by the surface for two main reasons, the broken cubic symmetry and the fact that the favored bulk hexaboride defects are metal vacancies that would give a hole excess rather than the observed electrons. We cannot give a unified or quantitative picture of how

this surface electronic structure comes about, but we can point to certain plausible ingredients for an explanation. It is thought [19] that the hexaboride [100] surface obtained by cleaving has a layer of metal atoms outermost as a result of breaking the inter-octahedra boron bonds. Band theory for SrB_6 shows [2] a variation in the X-point band overlap of 0.5 eV for only a 3.5% change in the x-parameter for fixed lattice parameter, in contrast to a very small change with varying lattice parameter for fixed x. The broken inter-octahedra bonds at the surface could allow the octahedra of a near-surface region to contract, which changes the x-parameter in the direction of restoring the X-point gap. As a related ingredient, the metal and boron octahedra are highly polar so that Coulomb energies could play a role in the largeness of the bandgap change. A surface of metal atoms is electron rich, consistent with our findings, and relative to the bulk a perfect such surface has 1 extra electron per cell with area density $\approx 1/16 = 0.0625\ \mathring{A}^{-2}$ for a cubic lattice constant $\approx 4\ \mathring{A}$. For the EuB_6 electron volume density of the surface region as estimated above from experiment, this number of electrons requires a surface region of thickness $\approx 0.0625/1\text{x}10^{-3} \approx 60\ \mathring{A}$, large enough to dominate the photoemission spectrum. The diffuseness of the closure of the FS image in Fig. 3(b) may well reflect some loss of translational symmetry in the perpendicular direction, arising from a variation of the x-parameter through this layer.

In summary our data provide the first global view of the electronic structure of the surprising divalent hexaborides. We validate the broad picture expected from band theory, including the important possibility of X-point bulk semi-metal FS, but with the surprise that for the surface region probed by ARPES, there is a large band gap, no X-point hole pocket, and a relatively large X-point electron pocket whose FS shape breaks cubic symmetry perpendicular to the surface. We speculate that the great sensitivity of the X-point gap to the x-parameter value plays an enabling role. By allowing the material to adjust and perhaps even to modulate its carrier densities, this sensitivity may well find its way into bulk properties, such as temperature dependences or inhomogeneity and phase separation effects of the kind discussed by Barzykin and Gorkov [12].

JWA expresses gratitude to M.C. Aronson for stimulating his interest in these materials, and to her and C. Kurdak for very enlightening discussions. This work was supported at U. of Michigan by the U.S. DoE under Contract No. DE-FG02-90ER45416 and by the U.S. NSF Grant No. DMR-99-71611. The Ames Lab is supported by the U.S. DoE under contract No. W-7405-ENG-82 and the SRC is supported by the U.S. NSF Grant No. DMR-95-31009.

* present address: Advanced Light Source, Lawrence Berkeley National Laboratory, Berkeley CA 94720
‡ present address: Physical Electronics, Inc., 6509 Flying Cloud Drive, Eden Prairie, MN 55344
† present address: Los Alamos National Laboratory, Los Alamos, NM 87545

[1] A. Hasegawa and A. Yanase, J. Phys. C, Solid State Phys. **12**, 5431 (1979).
[2] S. Massidda, A. Continenza, T. M. D. Pascale, and R. Monnier, Z. Phys. B **102**, 83 (1997).
[3] C. N. Guy, S. von Molnar, J. Etourneau, and Z. Fisk, Solid State Commun. **33**, 1055 (1980).
[4] L. Degiorgi *et al.*, Phys. Rev. Lett. **79**, 5134 (1997).
[5] J. C. Cooley, M. C. Aronson, J. L. Sarrao, and Z. Fisk, Phys. Rev. B **56**, 14541 (1997).
[6] P. Nyhus *et al.*, Phys. Rev. B **56**, 2717 (1997).
[7] S. Süllow *et al.*, to be published .
[8] H. R. Ott *et al.*, Z. Phys. B **102**, 337 (1997).
[9] D. P. Young *et al.*, Nature **397**, 412 (1999).
[10] M. E. Zhitomirsky, T. M. Rice, and V. I. Anisimov, Nature **402**, 251 (1999).
[11] L. Balents and C. M. Varma, Phys. Rev. Lett. **84**, 1264 (2000).
[12] V. Barzykin and L. P. Gor'kov, Phys. Rev. Lett. **84**, 2207 (2000).
[13] R. G. Goodrich *et al.*, Phys. Rev. B **58**, 14896 (1998).
[14] D. Hall, D. Young, Z. Fisk, and R. G. Goodrich, NHMFL Annual Report (1998).
[15] M. C. Aronson *et al.*, Phys. Rev. B **59**, 4720 (1999).
[16] C. O. Rodriguez, R. Weht, and W. E. Pickett, Phys. Rev. Lett. **84**, 3903 (2000).
[17] S. Massidda, R. Monnier, and E. Stoll, to be published .
[18] F. J. Himpsel, Adv. Phys. **32**, 1 (1983).
[19] R. E. Watson and M. L. Perlman, Surf. Sci. **122**, 371 (1982).

FIGURES

Fig. 1. Comparison of theoretical band structures (dashed lines) to experimental bands (reverse gray scale images and symbols) along Γ-X for (a) EuB_6 and (b,c,d) SrB_6 illustrating the ≈1.5 eV shift of the boron-derived bands relative to X-point electron pocket. Experimental data is for Γ-X parallel (a,b) and perpendicular (c) to the photon electric vector. Experimental SrB_6 bands from panels (b, c) are combined in (d) [diamonds and circles respectively].

Fig. 2. (a) k_x-k_y E_F intensity maps at hν=30 eV and (b) dispersing spectral lineshapes (hν=29.5 eV) along k_x at the X-point of EuB_6 and SrB_6.

Fig. 3. (a) X-point k_x-k_z E_F intensity map of EuB_6. (b) The same data normalized by the average intensity at each photon energy. White dots in (a) represent the experimental sampling density. Open circles in (b) show the k-point locations of the EDC's of Fig. 2 and of EDC's with varying hν, shown in panel (c). (d) Intensity representation of the EDC's in (c) normalized by the integrated spectral weight from 0.5 eV to E_F, and plotted with the same vertical k_z axis as in (b). Closed circles in (b) show FS locations from EDC E_F crossings.

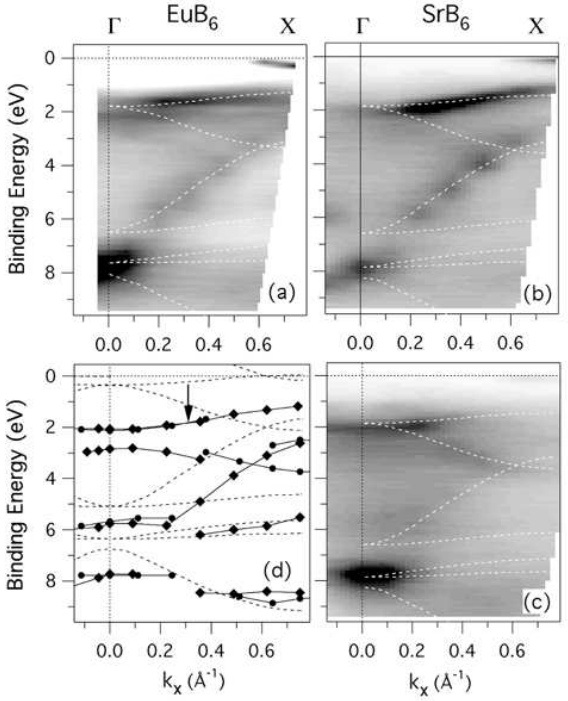

Fig. 1

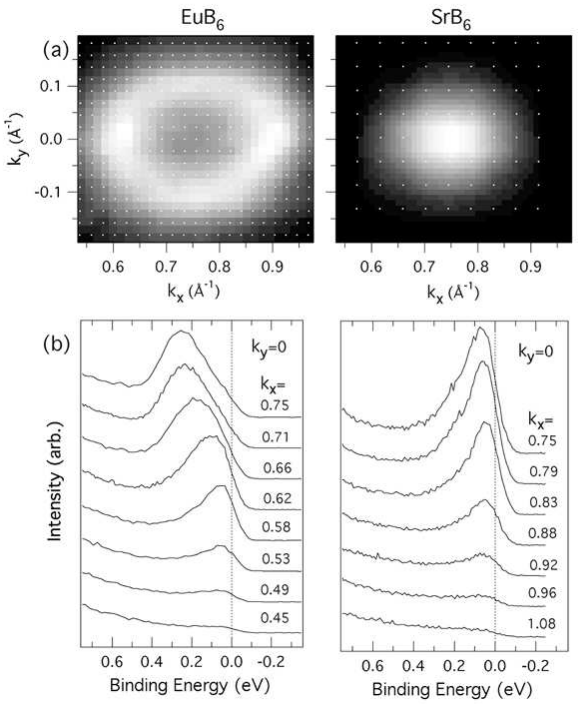

Fig. 2

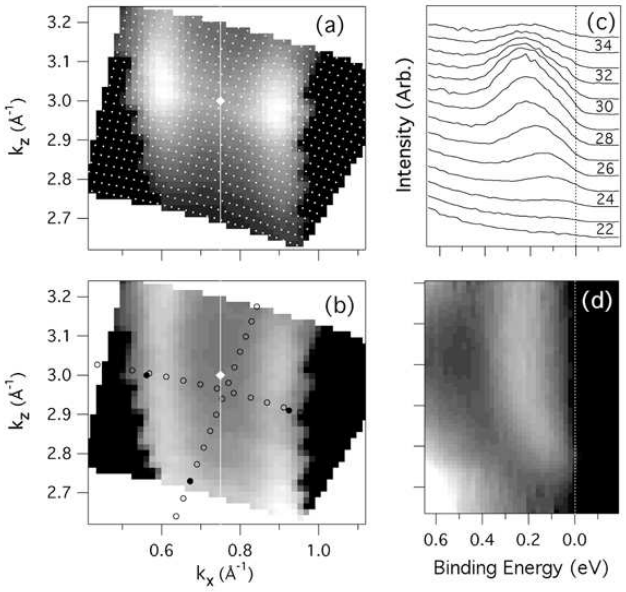

Fig.3